



# Tribological, Thermal and Corrosive Behaviour of Aluminium Alloy 2219 Reinforced by $\text{Si}_3\text{N}_4$ Nanosized Powder

C. J. Manjunatha<sup>1</sup> · B. Venkata Narayana<sup>2</sup> · D. Bino Prince Raja<sup>3</sup> · R. S. Rimal Isaac<sup>4</sup>

Received: 23 March 2021 / Accepted: 16 June 2021 / Published online: 29 June 2021  
© Springer Nature B.V. 2021

## Abstract

The Metal Matrix Composite (MMC) technique is the most effective contrast method when compared with other techniques. By using the method of high energy stir casting, Aluminium alloy Al2219 is reinforced with various percentages of  $\text{Si}_3\text{N}_4$  (0, 3, 6, and 9 %) particles. X-ray diffraction along with Scanning electron microscope was performed to characterize the composite. The mechanical and thermal behaviours such as differential thermal analysis thermo gravimetric analysis/, tensile, wear and hardness behaviours were investigated. By using electro chemical potentiodynamic polarization test, the consequence of heat treatment on the corrosion behaviour of the composites when compared to its matrix in 3.5 % NaCl when at 600 rpm was also investigated. In this experimental study, the wear of the aluminium composites was significantly decreased on addition of  $\text{Si}_3\text{N}_4$  particles. The study also revealed that, since the inclusion of  $\text{Si}_3\text{N}_4$  in the samples and compared to the base aluminium alloy, the mechanical properties of the composites, such as wear resistance, hardness and tensile strength increased by percentage. The surface morphology and Scanning electron microscope analysis of worn surfaces in the test pieces unfold that with the increase in reinforcement content, wear rate decreases.

**Keywords**  $\text{Si}_3\text{N}_4$  · Thermal analysis · Wear · Corrosion analysis · SEM

## 1 Introduction

In the recent times, the technology space in aircraft, aerospace, and automotive industries is rapidly advancing which in turn increases the demand for composite materials which is widely being used in the above-mentioned areas. The special properties of Composites materials such as low specific gravity makes the material highly superior in modulus and strength when compared with most traditional engineering metallic materials [1, 2].

Metal Matrix Composites (MMCs) are explicitly utilized composite materials which is made with generally two constituents, one of the constituents is a metal matrix and the other material is a reinforcement. In all the cases, the matrix is outlines with a metal and the use of pure metal as a matrix is mostly avoided. In general, the matrix is constituted by the use of an alloy. The general synthesis of the composite involves the mixing of the matrix and the reinforcement together.

Aluminium is extensively used in MMCs. This is main reason for this is the unique features of aluminium such as good mechanical properties, low density, good machinability properties, low electrical resistance, high strength and good corrosion resistance. Although comparatively substandard wear resistance of these alloy has restrained its use in specific tribological applications [3, 4]. In the recent studies, both particulate and fibre reinforced aluminium alloy composites fabricated have shown appreciable improvement in their tribological properties, including but not limiting to sliding wear, seizure resistance, friction, and abrasive wear [5, 6]. The production and utilization of  $\text{Si}_3\text{N}_4$  was stimulated by increasing demand for low-cost reinforcement [7–9].

---

✉ C. J. Manjunatha  
manjunathacj79@gmail.com

<sup>1</sup> Department of Mechanical Engineering, Sha-Shib College of Engineering, Vtu, Chickballapur, India

<sup>2</sup> Department of Mechanical Engineering, Sea College of Engineering, Bangalore, India

<sup>3</sup> Department Of Aeronautical Engineering, SJC Institute of Technology, Chickballapur, India

<sup>4</sup> Department of Nanotechnology Noorul Islam Centre for Higher Education, Kanyakumari, Tamil Nadu, India

Wear based damages to the material is an important aspect in tribology but even though it is highly important, it is one of the least understood fields. It is also a youngest topic, lubrication, friction and wear which needs more scientific attention. The practical significance of the same is being identified through the years [10–12].

Wear is responsible for a huge annual outlay by the consumers as well as the industries. Most of this goes in replacing or repairing equipment's that is worn out and does no longer perform its function [13]. In many parts of the machine the damage is seen only after a percentage of the entire volume of the part has worn out [14, 15].

Number of studies have been conducted to characterize tribological behavior of Aluminium-based MMC. Suresh and Sridhara [16] reported on the impact of Gr and SiC (up to 10 % wt%) on the wear properties of LM25-based aluminium composites. It was discovered that increasing the weight fraction of reinforcement particle in MMC reduced wear until it reached 7 %, after which it increased. Wear of matrix material composites increased with increasing load due to an unstable tribo-layer, but decreased with increasing speed due to the presence of Mechanically Mixed Layer (MML) [17]. The effect of SiC and B<sub>4</sub>C on the wear efficiency of the Al7075-based MMC was studied by Uvaraja and Natarajan [18]. Wear rate was found to decrease as the volume fraction of reinforcement, speed, and time increased, whereas it increased as the applied load increased. The reinforcement content was found to be the most important factor, followed by the applied load and sliding speed. Surface morphology and SEM analysis of the test pieces' worn surfaces showed that the wear rate decreased as the reinforcement material increased. The EDS findings were used to classify the MML that forms on the test specimen's worn surfaces [19, 20]. The zinc effect on the microstructure was investigated by keeping the ratio of zinc in the mixture at different ratios for each mixture. X-ray diffraction (XRD) analysis was carried out to investigate the different phases. Analyses of the microstructures of alloys with different alloying times were investigated by scanning electron microscopy (SEM) and optical microscope [21, 22].

The effects of reinforcement on composite corrosion activity are still unknown. It has been found that in the presence of reinforcement, the corrosion current density rises, decreases, or remains unchanged. Furthermore, reinforcement has been shown to influence the open circuit potential (OCP) by increasing, decreasing, or having no effect [23, 24]. Heat treatment results are discovered to be a crucial factor in evaluating the corrosion behaviour of aluminium alloy composites. Kolman and Butt [25, 26] examined the corrosion properties of an aluminum–silicon alloy composite reinforced with in-situ TiB<sub>2</sub> particulate after heat treatment. It was discovered that as the amount of TiB<sub>2</sub> in these composites increased, their corrosion resistance decreased. The effect of heat treatment of the reinforcing BN, Al<sub>2</sub>O<sub>3</sub>, and Ti (C, N) particles in the EN

AW–AlCu4Mg1(A) aluminium alloy on its corrosion resistance in the presence of NaCl water solution was investigated by Wodarczyk-Fligier et al. [27, 28]. The corrosion resistance of composite material heat treated in a 3 % NaCl solution was found to be noticeably improved [29]. The tensile strength of the samples decreases, the elongation of the extruded samples increases. Consequently, reciprocating extrusion is an effective method for improving the mechanical properties of metal matrix composites (MMC) [18, 30].

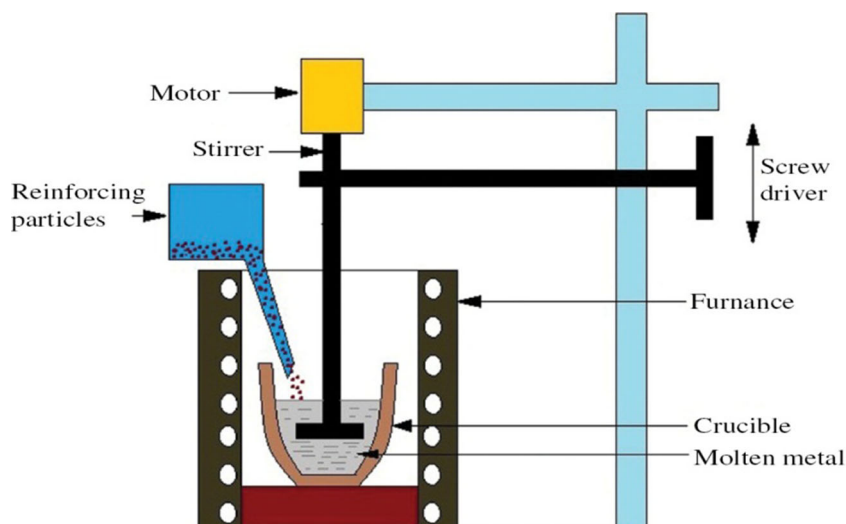
In the context of the above discussion, it has been found that no work has been carried out by the combination of Al2219/Si<sub>3</sub>N<sub>4</sub> with different composition. Also, characterization such as TGA, Corrosion have not been conducted by other researchers. So, the aim of the present work is to study the Tribological, Thermal and Corrosive behaviour of aluminium alloy 2219 reinforced by Si<sub>3</sub>N<sub>4</sub> nanosized powder. The reinforcement is embedded by high energy stir casting method with various percentage of Si<sub>3</sub>N<sub>4</sub> (0,3,6 and 9) particles. The structural characterization was carried out by SEM and XRD tests. Tensile, hardness and corrosion test are carried out for determining the mechanical behaviour of this material. TGA analysis has been carried for the purpose of thermal analysis. The wear behaviour of AA2219/ Si<sub>3</sub>N<sub>4</sub> MMC has not been explored so far and they are fabricated by two-step stir casting method. Characterization of microstructure and worn surface morphology of the composites was done by Scanning electron microscope (SEM). Tensile fractured samples were made to undergo fractography study. Mechanically mixed layer (MML) of the test specimens were evaluated by EDS.

## 2 Experimental Aspects

### 2.1 Casting Process

In this study the electrical furnace setup was replaced with a stir set up by using a simple blower furnace and the vertical drilling machine assembly as shown in the Fig. 1. As the high operating cost of electrical furnace is annihilated, the variable speed of drilling machine is obtained using the stirrer. The addition of Si<sub>3</sub>N<sub>4</sub> particles in terms of ratio was done at 0, 3, 6, and 9% by the overall weight. Formulation process begins with the stirring out in a graphite crucible in a coal-fired furnace. Ceaseless stirring of the molten metal-matrix gives homogeneous mixture of the composite. This is instantly poured into the mould to get solidified. For melting the alloy Coal was used as a fuel. Al2219 was kept in a crucible and liquefied by melting it in a blower furnace at a temperature of 670°C for 15 min. The Si<sub>3</sub>N<sub>4</sub> powder was preheated to a temperature of 670 °C using a separate muffle furnace. The temperature of the furnace was first increased above the temperature of the liquid.

**Fig. 1** Typical stir-casting experimental setup



**2.2 Tensile Test**

Ductile test examples were made according to the ASTM standard and tried in a Universal Testing Machine. In request to gauge the rigidity of the examples, they were made in a round and hollow shape as per ASTM E8. The information estimations of the four examples acquired from the ductile test were utilized. The fortifying stage in the metal network composites bears a huge division of the worry as it is commonly a lot stiffer than the grid. The molecule joining brings about an expansion in the work solidifying of the material. The higher work solidifying rate saw in the composites is because of the mathematical imperatives forced by the presence of the support. The expanding weight % of  $Si_3N_4$  builds the work solidifying rate. The tensile samples before and after test is shown in Fig. 2(a) and (b).

**2.3 Hardness Test**

The composites materials hardness was estimated by utilizing a Brinell hardness machine following the ASTM E10

standard. All the examples were applying a heap of 500 to 3000kgf for a time of Ten seconds. The test was done at room temperature and the estimation of hardness was taken at 3 distinct areas to keep away from the conceivable impact of indenter laying on the hard support particles. The midpoints of the apparent multitude of four readings were accounted for.

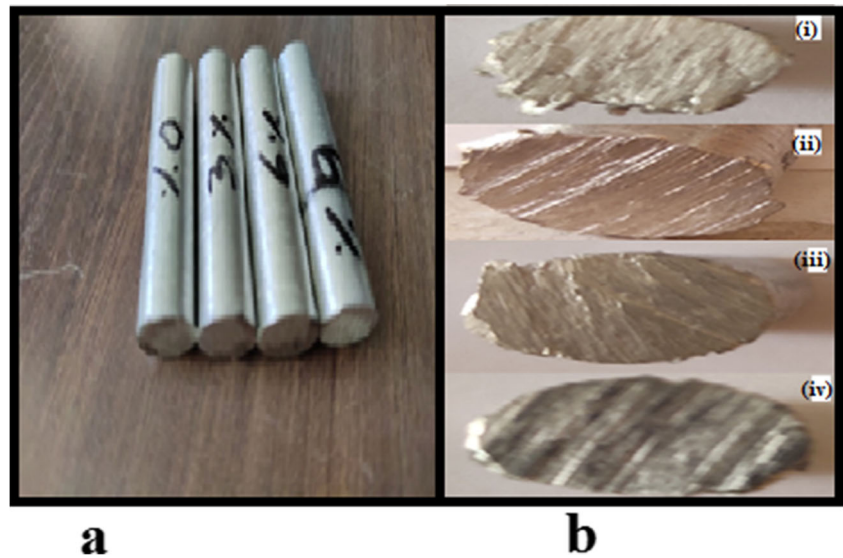
**2.4 Pin-on-disc Experimental Set Up**

A pin-on-disc equipment is used to carry out the experiment which is coupled with a wear monitor and type friction with a data acquisition system. The above setup is used in measuring the wear behavior of composite by testing it against the hardened ground steel disc (EN-24) which is has a hardness value of 65HRC and surface roughness (Ra) of 0.5  $\mu m$ . the equipment is highly versatile which is designed in such a way to study the wear characteristics only under sliding conditions. In the equipment, sliding usually occurs between the rotating disc and the stationary pin. A D.C motor was used to rotate the disc; the motor is having a speed range of 100–1500 rpm with wear track diameter (50mm\*160mm), which would yield

**Fig. 2** Tensile test specimen before testing (a) and after testing (b)



**Fig. 3** Wear specimens (a) Before & (b) After test



sliding speed 0 to 10 m/sec. The load has to be applied on pin sample (specimen) by deadweight through a pulley string arrangement. The system's maximum loading capacity is 100 N. Figure 3(a) & (b) shows Wear specimens before and after test.

## 2.5 TGA

Differential thermal analysis (DTA) and thermogravimetric analysis (TG) were carried out simultaneously using a TG/DTA EXSTAR 6300 instrument (SII Nanotechnology Inc.). Approximately 10 mg of the specimen is weighed on the alumina crucible and heated from 30 to 800 °C in a flow of air atmosphere (100 ml/min). The heating rate was 10 °C/min.  $\alpha$ -Alumina was used as reference standard.

## 2.6 XRD

XRD is commonly utilized to assess the samples' purity, phase and crystal structure [25]. Phase analysis of prepared specimens was done by XRD model D2 PHASER (Bruker AXS) using Cu/K $\alpha$  radiation ( $\lambda = 1.54060 \text{ \AA}$ ). Over the  $2\theta$  range of  $20^\circ$ – $80^\circ$  with a step size of  $0.02^\circ$ , peak values were obtained. Different shapes correspond to a different growth of crystal structures resulting on different intensities of the XRD peaks.

Characteristics peaks has been observed in the XRD pattern, and the relative intensity rate corresponding to the samples.

## 2.7 Corrosive Test

Corrosion measurement were carried out using CHI 604D Electrochemical Workstation (CH Instruments, Inc) in 3.5 % NaCl Solution using an Ag/AgCl reference electrode and

**Fig. 4** Corrosion samples





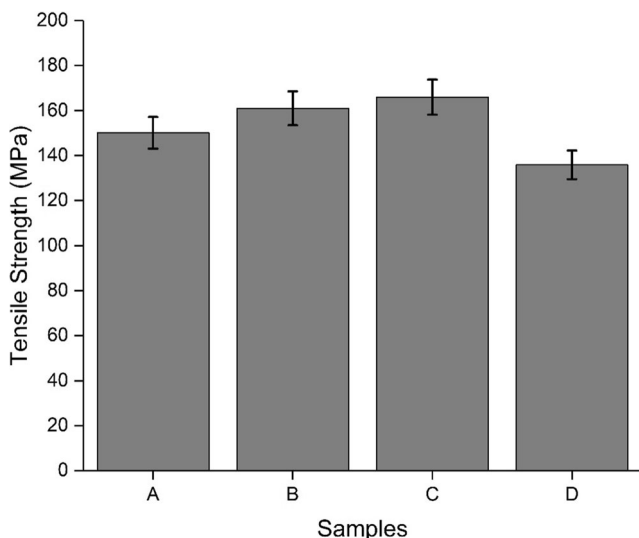


Fig. 5 Effect of tensile strength on wt% of Si<sub>3</sub>N<sub>4</sub>

platinum wire as a counter electrode. The Inhibitive efficiency is calculated using the below Eq. (1).

$$Inhibition\ Efficiency = \frac{C_{ra} - C_{rs}}{C_{ra}} \times 100 \quad (1)$$

In the above equation for Inhibition Efficiency, C<sub>ra</sub> denotes the corrosion rate of the unreinforced Al2219 alloy and C<sub>rs</sub> is used to denote the corrosion rate of Al2219 alloy reinforced with Si<sub>3</sub>N<sub>4</sub>. Each run’s output consists of a polarisation curve from which the corrosion parameters can be calculated using a manufactured software package using the Tafel extrapolation technique. The samples are shown in Fig. 4.

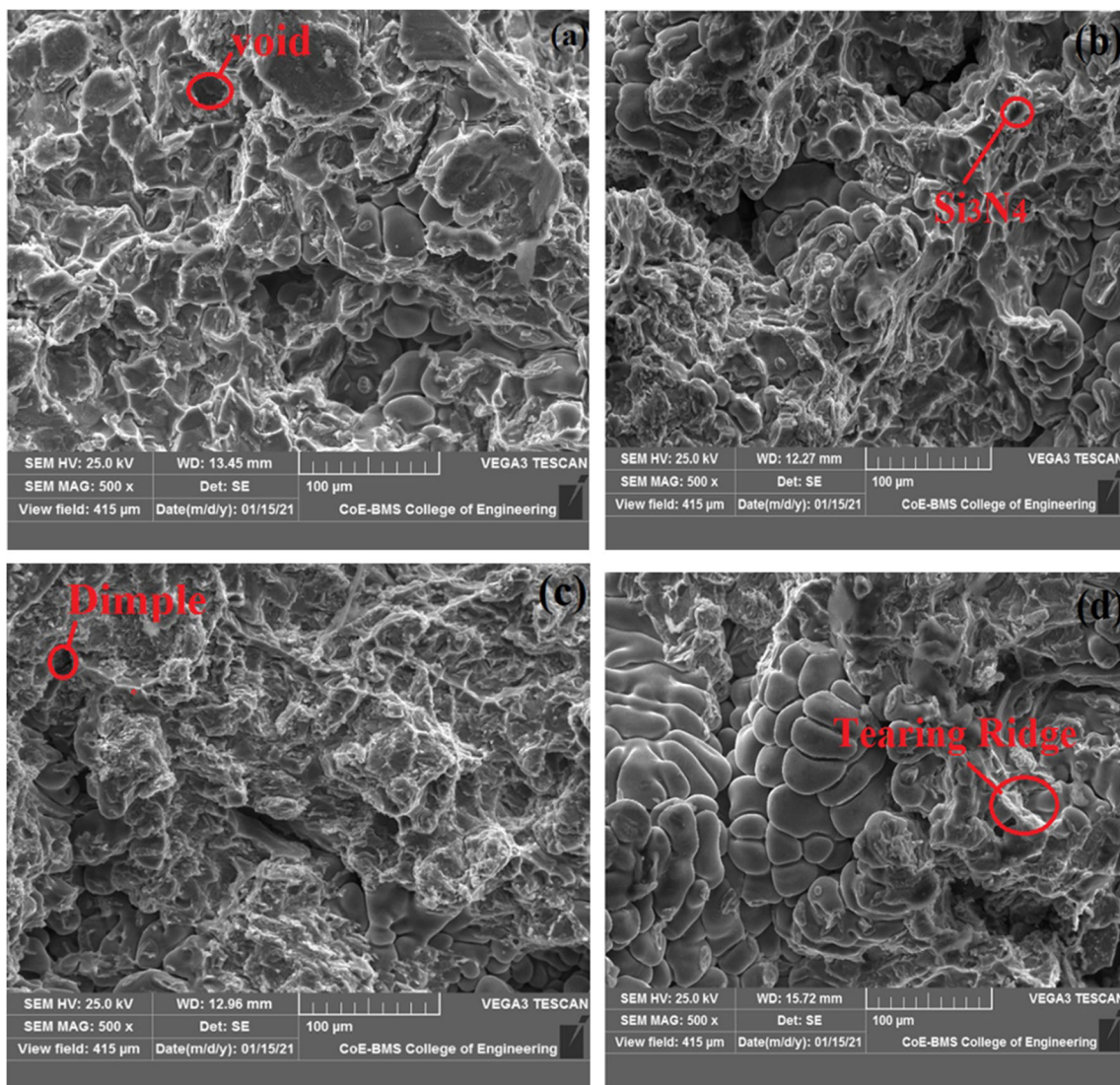


Fig. 6 (i): Fractography of Al 2219 Alloy + 0 % Si<sub>3</sub>N<sub>4</sub>. (ii): Fractography of Al 2219 Alloy + 3 % Si<sub>3</sub>N<sub>4</sub>. (iii): Fractography of Al 2219 Alloy + 6 % Si<sub>3</sub>N<sub>4</sub>. (iv): Fractography of Al 2219 Alloy + 9 % Si<sub>3</sub>N<sub>4</sub>

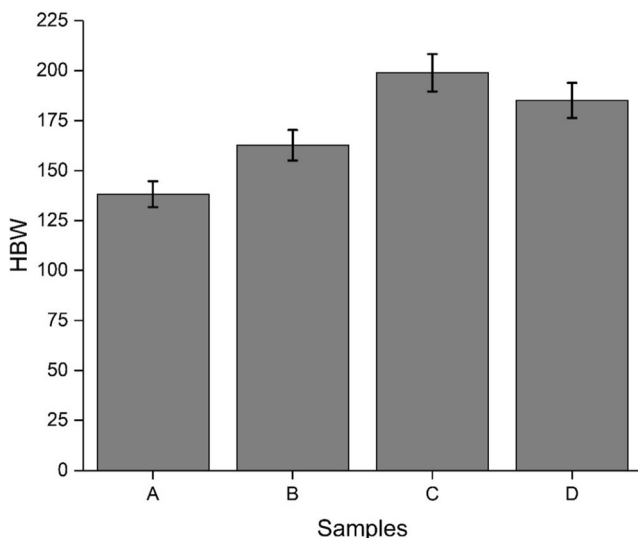


Fig. 7 Effect of hardness on wt% of Si<sub>3</sub>N<sub>4</sub> particles

### 3 Result & Discussion

#### 3.1 Effect of Tensile Analysis

Mechanical conduct of the composites was explored by pliable tests which are done utilizing a mechanized widespread malleable testing machine. The examples when the ductile test has appeared in Fig. 5. Four test examples were utilized for each run. The malleable properties, for example, rigidity, extreme elasticity, and modulus were deciphered from the pressure strain bends spoke. It is additionally obvious from the malleable test that expansion in the measure of support builds the elasticity, whereas there exists a lessening in pliability huge enhancement in the mechanical properties of the composite as contrasted and the Al2219 can be ascribed to the Si<sub>3</sub>N<sub>4</sub>.

The tensile tested specimen of AA2219 alloy with 0 %, 3 %, 6 and 9 % of Si<sub>3</sub>N<sub>4</sub> reinforced composite is subjected

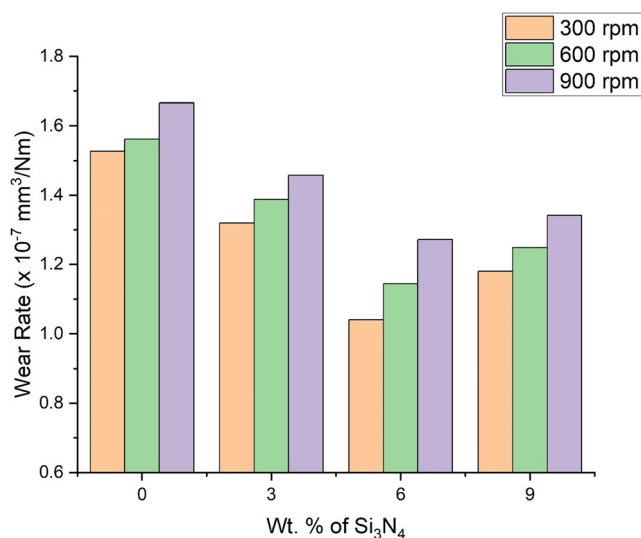


Fig. 8 Wear rate vs. Wt. % of Si<sub>3</sub>N<sub>4</sub> (load: 20 N)

to fracture morphology and the result is as shown in Fig. 6(i-iv). It has been noted that sample with 3 % wt demonstrated a high breakage point. Scanning electron microscope image of AA2219 alloy in the Fig. 6(i-iv) unravels that the AA2219 alloy has equally distributed, large voids, with a good number of comparatively equalled fibrous ligaments and dimples present on its surface. This discloses the ductile mode of the fracture. The composites 0 %, 3 %, 6 and 9 % of Si<sub>3</sub>N<sub>4</sub> as shown in figure are small and minimal. Within the dimples the Si<sub>3</sub>N<sub>4</sub> particles are excellently harboured. This confirms a good bonding between the matrix and the Si<sub>3</sub>N<sub>4</sub> [30]. Because of the existence of Si<sub>3</sub>N<sub>4</sub> particles, the dimples were found to be much shallower, and their size was decreased by growing a fraction of Si<sub>3</sub>N<sub>4</sub> particles. This shows that the particles are uniformly distributed and strongly bound to the matrix. Despite the fact that fracture morphology shows signs of ductile fracture, ductile fracture is heavy in the AA2219 alloy and low in the composite. These fractography clearly demonstrate that the matrix and reinforcement have a strong bond, resulting in improved composite hardness and ultimate tensile strength [13, 30]. It confirms that as the percentage of Si<sub>3</sub>N<sub>4</sub> increases, the percent of elongation decreases. This is mostly due to the Si<sub>3</sub>N<sub>4</sub> particle's hardness. Many other researchers have found similar patterns [1, 13, 21, 30].

#### 3.2 Brinell Hardness Analysis

The after-effects of Brinell hardness tests directed on AA2219 and the composite containing diverse wt% of Si<sub>3</sub>N<sub>4</sub> particles have appeared in Fig. 7. They uncover critical improvement in the hardness with the expansion of Si<sub>3</sub>N<sub>4</sub> fortification in the AA2219. The AA2219 composite with hardness esteem 63.71 HV and the aluminium-based composite containing 2 wt% Si<sub>3</sub>N<sub>4</sub> demonstrates 65.39 HV and this goes with expanding Si<sub>3</sub>N<sub>4</sub> content. It is seen that the hardness of 10 % Si<sub>3</sub>N<sub>4</sub> is expanded by 73.93 HV more than AA2219. A striking accent in the hardness of the composite network can be seen with the expansion of Si<sub>3</sub>N<sub>4</sub> particles. Hardness esteem uncovers that

Table 1 Wear rate of all the samples with 20KN and 40KN Load

Load (N)	Sliding speed (Rpm)	Wear rate in 10 <sup>-7</sup> mm <sup>3</sup> /Nm			
		Wt.% of Si <sub>3</sub> N <sub>4</sub>			
		0	3	6	9
20	300	1.527	1.319	1.041	1.180
	600	1.562	1.388	1.145	1.249
	900	1.666	1.458	1.272	1.342
40	300	2.013	1.527	1.458	1.527
	600	2.326	2.152	1.701	1.874
	900	2.430	2.360	1.944	2.129

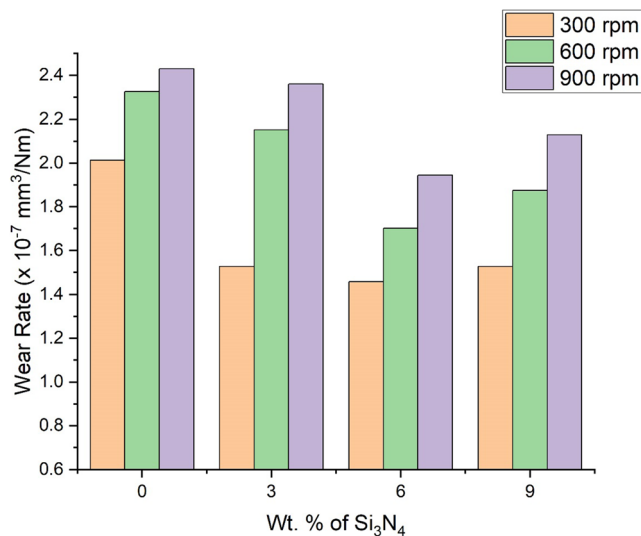


Fig. 9 Wear rate vs Wt. % of Si<sub>3</sub>N<sub>4</sub> (load: 40 N)

the higher estimation of hardness demonstrates the presence of Si<sub>3</sub>N<sub>4</sub> particulates in the lattice composites. A hard fortification is consolidated into a delicate material; the hardness of the grid material is enhanced. Consequently, expanding the wt% of Si<sub>3</sub>N<sub>4</sub> builds the hardness of the composites.

### 3.3 Effect of Wear Analysis

The above Fig. 8 shows effect of wt% of Si<sub>3</sub>N<sub>4</sub> and sliding speed on wear behaviour of the AA2219/Si<sub>3</sub>N<sub>4</sub> composites at 20 N. Table 1 shows the Wear rate of all the samples with 20KN and 40KN Load.

The above Fig. 9 shows the Effect of wt% of Si<sub>3</sub>N<sub>4</sub> and with sliding speed of disk on wear behaviour of the Al2219/Si<sub>3</sub>N<sub>4</sub> composites at 40 N. The effect of Silicon Nitride (Si<sub>3</sub>N<sub>4</sub>) content on the wear characteristics of AA 2219/Si<sub>3</sub>N<sub>4</sub> particulate for a wear test the loads of 20, and 40 N and rotational speed of 300, 600, and 900 rpm as shown in Figs. 7 and 8 which is the representative graphs plotted based on wear rate results. The following is revealed by the study of these Figures. The wear rate of the AA 2219/Si<sub>3</sub>N<sub>4</sub> composites depends on the % of Silicon Nitride (Si<sub>3</sub>N<sub>4</sub>) dispersion. With the increase in Silicon Nitride (Si<sub>3</sub>N<sub>4</sub>) content from 3 to 6 wt% wear rate was found to be decreased. But there is a result of an increase in wear rate for the 9 wt% of Silicon Nitride (Si<sub>3</sub>N<sub>4</sub>) when compared with the 6 wt% reinforcement. The weighted rate by wear is minimum for the composite containing 6 wt% Silicon Nitride (Si<sub>3</sub>N<sub>4</sub>) dispersed in the as-cast as observed. At lower loads, the wear rate of the material remained almost constant with an increase in rpm. When comparing the results,

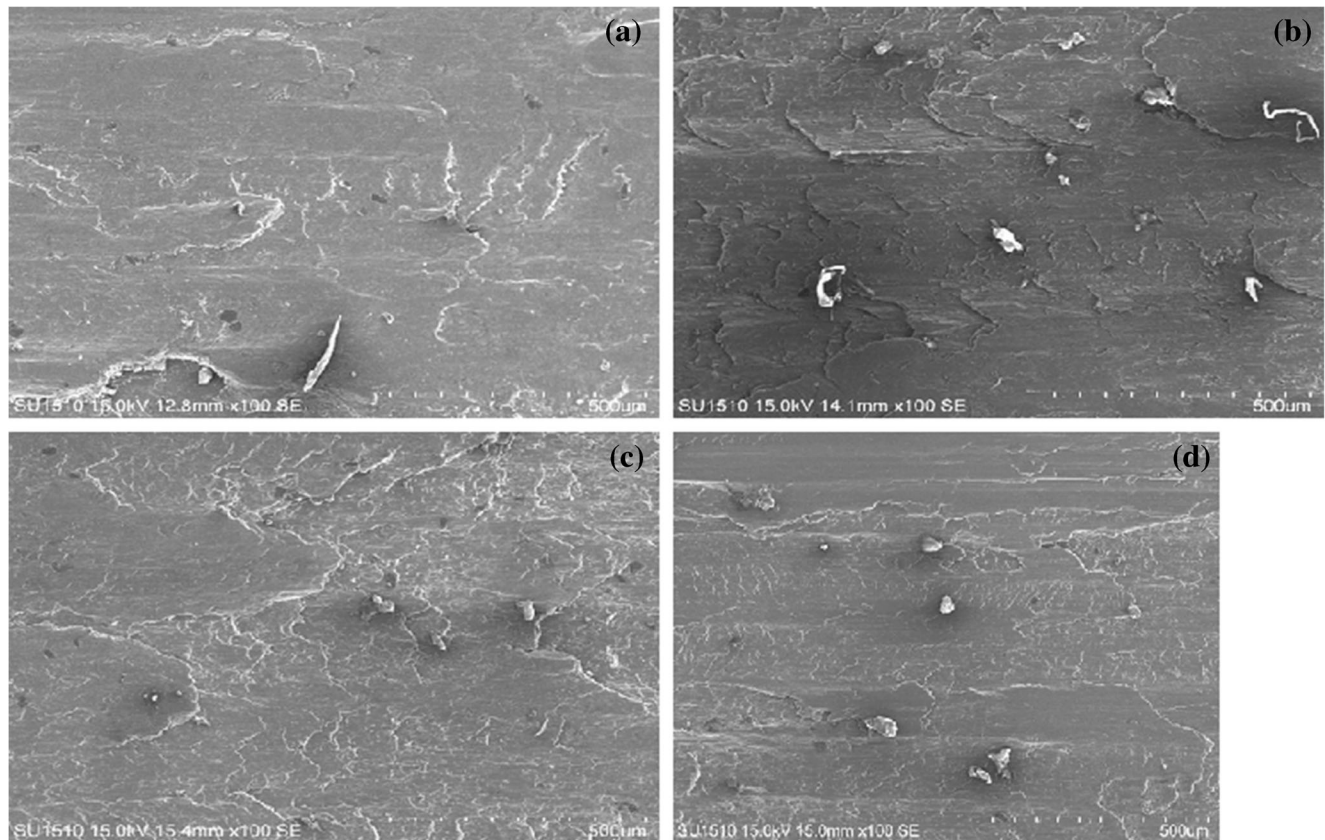
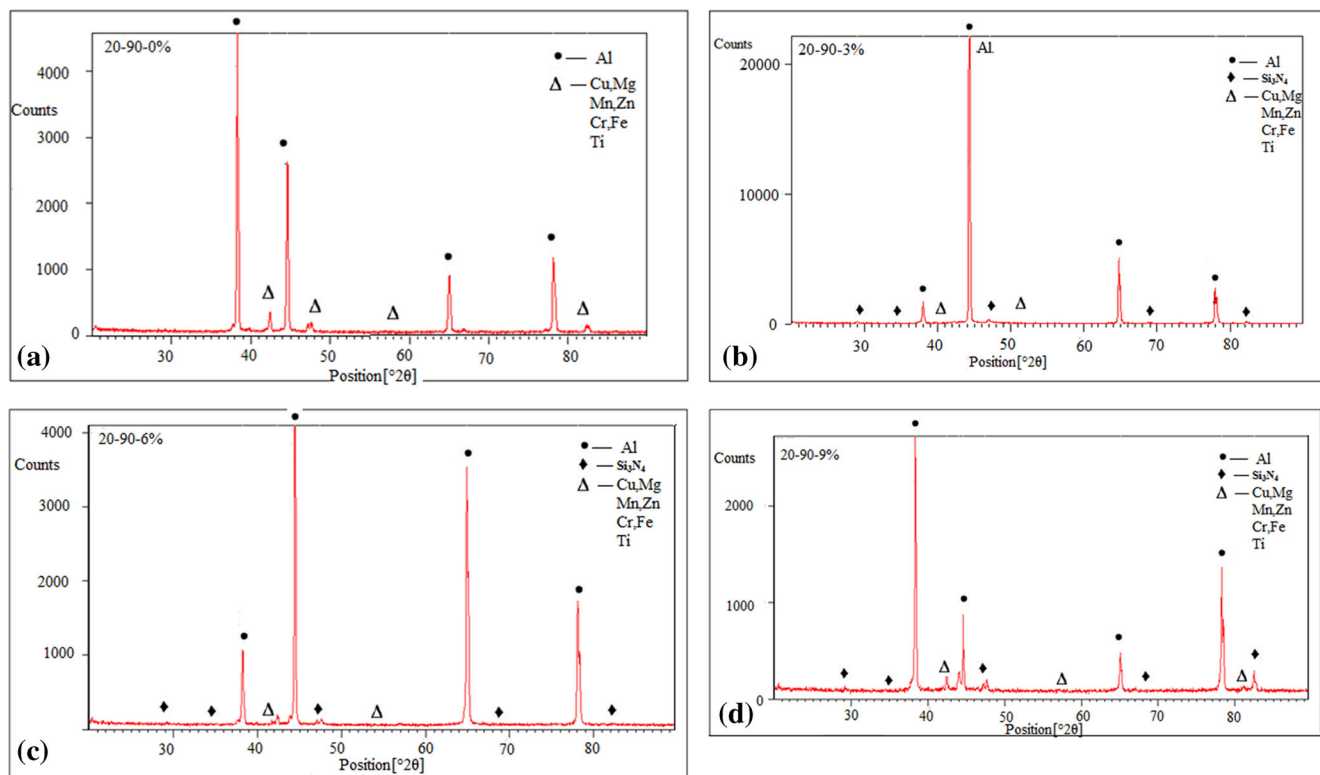


Fig. 10 (a): SEM micrographs of the worn surface of specimen for 0 %. (b): SEM micrographs of the worn surface of specimen for 3 %. (c): SEM micrographs of the worn surface of specimen for 6 %. (d): SEM micrographs of the worn surface of specimen for 9 %





**Fig. 11** (a): XRD pattern of as casted AA2219 (0 %). (b): XRD pattern of AA2219 + 3 wt %  $\text{Si}_3\text{N}_4$ . (c): XRD pattern of AA2219 + 6 wt %  $\text{Si}_3\text{N}_4$ . (d): XRD consequence of AA2219 + 9 wt %  $\text{Si}_3\text{N}_4$

the light wear rate was shown by AA2219 without dispersoid loss decreased in a steady manner. Perhaps, due to hard particles of Silicon Nitride ( $\text{Si}_3\text{N}_4$ ) dispersed in the base matrix there is relatively rapid attainment of stability in the wear resistance, as seen in the above figures.

### 3.4 Worn Out Surface Analysis of Wear Specimens

Figure 10(a) – (d) shows the surfaces of samples as viewed using a SEM which is cast Al2219 alloy and Al2219-3,6,9 wt%  $\text{Si}_3\text{N}_4$  composites after applying a load of 20 N, 40 N and 300, 600, 900 rpm sliding speed test. Figure 10(a) shows that some of the regions are damaged as seen in as cast Al2219 alloy. When higher load was applied, the degree of grooves formed at the worn surface of the matrix alloy is quite larger which causes a severe plastic deformation which causes severe wear in the specimens. Figure 5.2, 5.3, 5.4 shows the amount of grooving in the surfaces of the Al2219 alloy composite. The grooves reduce as a result in the increase content of  $\text{Si}_3\text{N}_4$  showing the lower material removal in comparison with Al2219 base matrix material.

### 3.5 XRD Investigations

Figure 11(a) shows the X-ray patterns of extracted AA2219 as cast composites. The fabricated AA 2219's X-ray diffraction pattern. The presence of aluminium (Al) and copper (Cu) of

metallic compounds was discovered through the study of XRD peaks. The diffraction pattern clearly indicates  $\text{Si}_3\text{N}_4$  particles, as shown in Fig. 11(b, c, and d). The relative fractions of the strength of the  $\text{Si}_3\text{N}_4$  particles were measured. The relative fractions of  $\text{Si}_3\text{N}_4$  particles found strength in the XRD pattern, with the highest peak occurring at the reinforcement particles. The particle peaks within the composite are visible using XRD. As the number of  $\text{Si}_3\text{N}_4$  particles increases, the probability of reinforcement agglomeration in the AA 2219 matrix increases. The results show that metallic elements are present in the highest peaks and reinforcement is present in the lowest peaks. The relative strength occurs at a 38-degree angle, with strong peaks for wt% of composites. The percentage of  $\text{Si}_3\text{N}_4$  in composites has been found to increase, resulting in a higher peak intensity level in the study.

### 3.6 TGA Analysis

Analyzing the thermal response of unreinforced Al2219 and developed Al2219-  $\text{Si}_3\text{N}_4$  composites as shown in Fig. 12(a-d), has been established using a differential thermal analyzer (DTA) and thermogravimetric analyzer (TGA). The results from the thermograms shows that as the composite with incorporated  $\text{Si}_3\text{N}_4$  has enhances the thermal stability of the aluminium alloy matrix. Apart from increase in inhibition efficiency, the addition of the nanoceramic  $\text{Si}_3\text{N}_4$  also causes a decrease in the mass loss as the composite is heated from 30



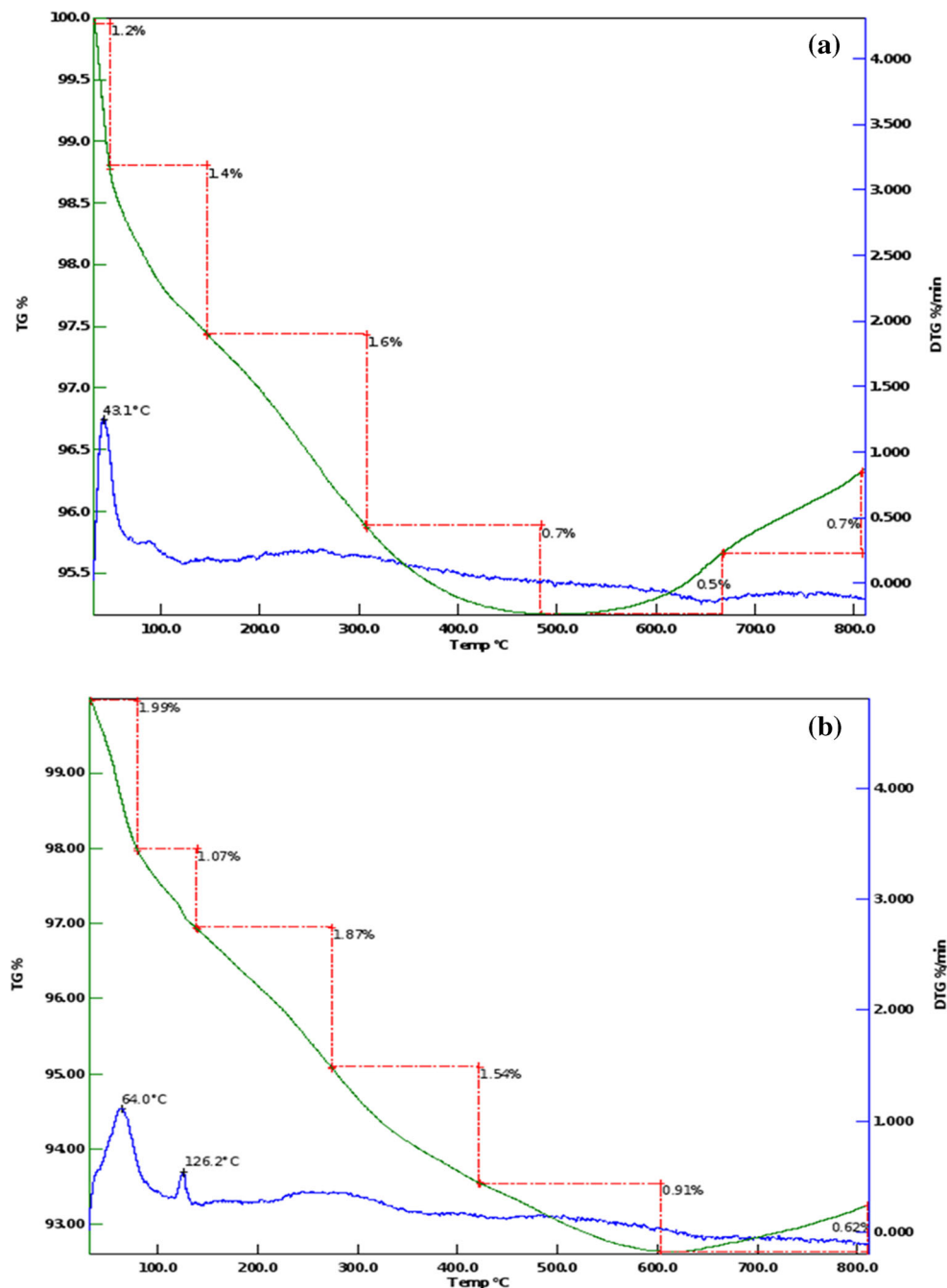


**Fig. 12** (a): TGA/DTG of AA2219 + 0 wt %  $\text{Si}_3\text{N}_4$ . (b): TGA/DTG of AA2219 + 3wt %  $\text{Si}_3\text{N}_4$ . (c): TGA/DTG of AA2219 + 6 wt %  $\text{Si}_3\text{N}_4$ . (d): TGA/DTG of AA2219 + 9 wt %  $\text{Si}_3\text{N}_4$

to 800 , which is clearly evident from the TG/DTA result. From the graph, there was a 7.3 % loss of mass for the unreinforced Al2219, whereas the addition of the incorporation of  $\text{Si}_3\text{N}_4$  decreased the mass loss to 2.5 % in 3 wt%  $\text{Si}_3\text{N}_4$  reinforced alloy. At 6 wt %- $\text{Si}_3\text{N}_4$ , the material was about 4.4 % and mass loss was observed in 9 wt% particulates with an 7.6 % loss. This shows the positive effect of the inclusion of the  $\text{Si}_3\text{N}_4$  helped in material saving for high temperature application by enhancing the reduction of mass loss with an optimal  $\text{Si}_3\text{N}_4$  amount of 3 %.

### 3.7 Corrosion

Figure 13 shows the potentiodynamic polarization graph for the Al 2219 allow with and without  $\text{Si}_3\text{N}_4$  reinforcement. From the results, the corrosion rate and the inhibition efficiency were calculated and is shown in Table 2. the results clearly shows that the corrosion rate decreases as with the addition of  $\text{Si}_3\text{N}_4$  which shows its positive effect on the material in preventing it from getting corroded. The inert properties of the nano ceramic  $\text{Si}_3\text{N}_4$  that makes it resistant to corrosion

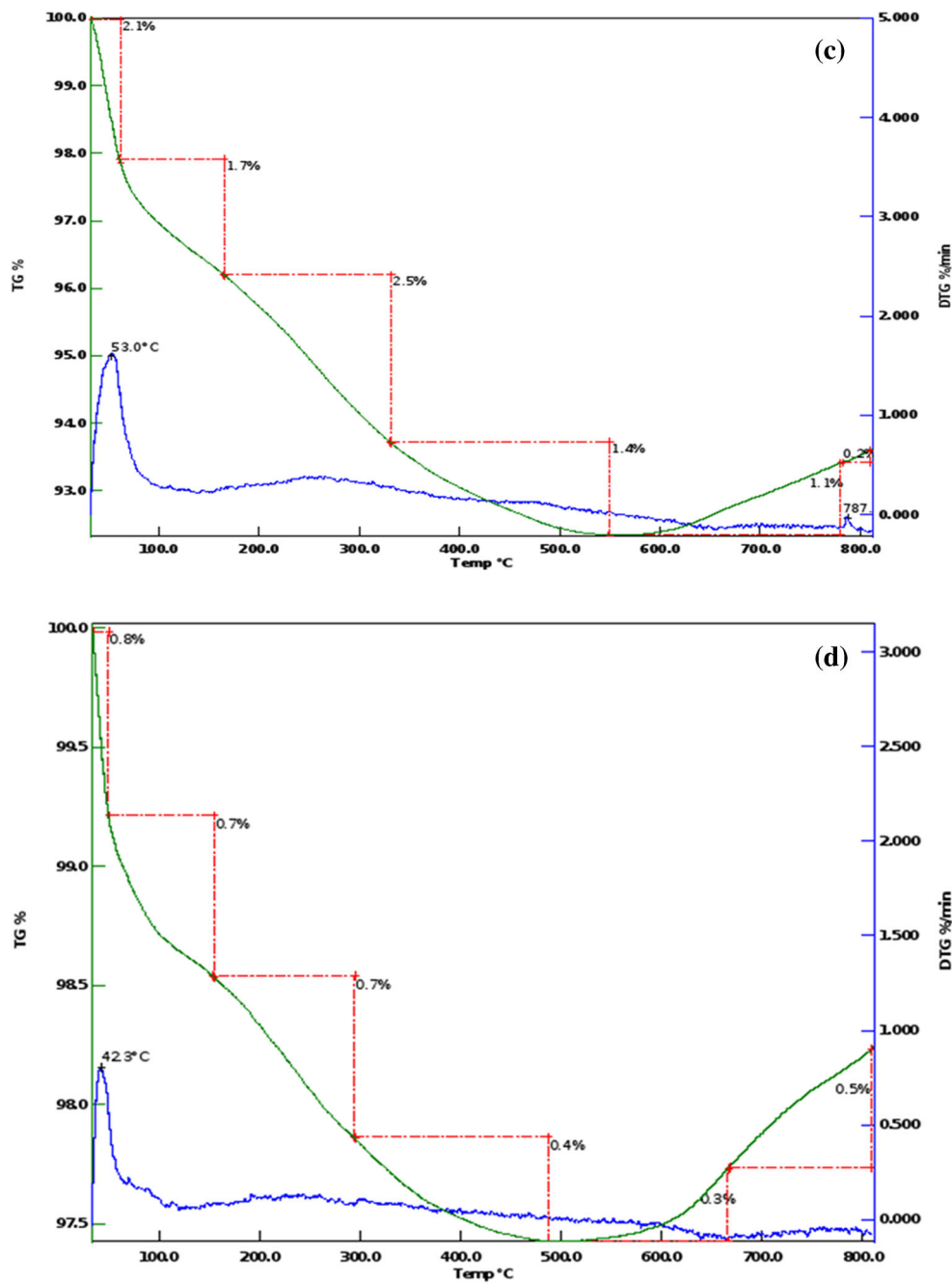


Fig. 12 (continued)

was seen to influence the composite to have a low corrosion rate, its positive effect on the corrosion inhibition efficiency increases as the  $\text{Si}_3\text{N}_4$  percentage increases from 3 to 9 %.

## 4 Conclusion

The tribological, thermal, morphological and mechanical characterisation of AA2219 reinforced with four wt% of  $\text{Si}_3\text{N}_4$  composite was made by stir casting method. The study revealed the following results:

- Due to the dispersion of  $\text{Si}_3\text{N}_4$  particles over the Aluminium alloy 2219, matrix increases the hardness value of the composites. Tensile strength increases firstly from 0 to 6 %  $\text{Si}_3\text{N}_4$  and decreases suddenly at 9 %  $\text{Si}_3\text{N}_4$ . HBW of the material gradually increases as percentage composition of aluminium varies from 0 to 6 %  $\text{Si}_3\text{N}_4$  and decreases in 9 % of  $\text{Si}_3\text{N}_4$ .
- Tensile strength of AA2219- $\text{Si}_3\text{N}_4$  composite revealed that high strength is obtained at 6 %wt addition of  $\text{Si}_3\text{N}_4$  when compared to other the weight %. The intensity of facts initial will increase from 0 to 6 % and then suddenly

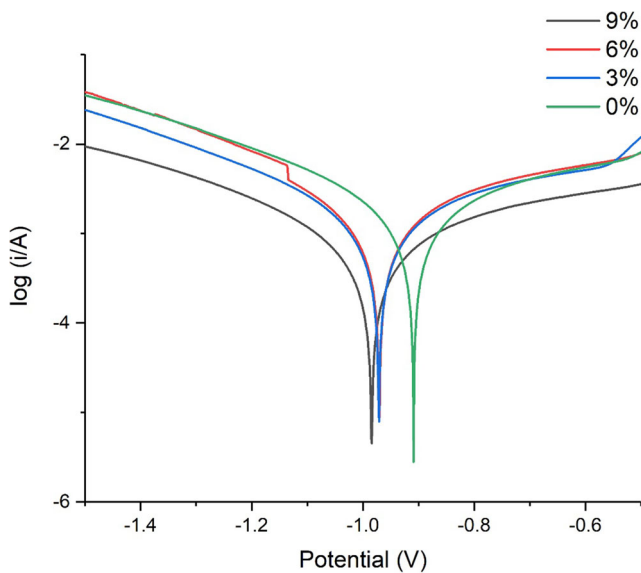


**Fig. 13** Polarization curves for Al–Si<sub>3</sub>N<sub>4</sub> alloy matrix and its composites with different wt% of Al<sub>2</sub>O<sub>3</sub> particles tested in 3.5 % NaCl

to 9%. The results of the tests like hardness and tensile increased with increasing the wt% of Si<sub>3</sub>N<sub>4</sub> in AA2219 composites [10].

- The XRD analysis of Al 2219 alloy / Si<sub>3</sub>N<sub>4</sub> composites reexhibits the aluminium, Silicon Nitride (Si<sub>3</sub>N<sub>4</sub>) and intermetallic (Al-Cu) phases.
- The tribological characteristics mass wear, friction force and coefficient of friction, of the AA2219-Si<sub>3</sub>N<sub>4</sub> composites increases with the 9% of Si<sub>3</sub>N<sub>4</sub> reinforcement. The AA2219-with 0,3, 6, and 9 wt% of Si<sub>3</sub>N<sub>4</sub> composites has shown the lower rate wear compared to the original AA2219 alloy matrix. Work concluded that the 9% of Si<sub>3</sub>N<sub>4</sub> reinforcement is better for the wear resistances at minimum load applications of Aluminium alloy 2219 matrix materials, the minimum amount of 6% of Si<sub>3</sub>N<sub>4</sub> reinforcement is to be suggested.
- The coefficient of friction and wear rate the of Al/ Si<sub>3</sub>N<sub>4</sub> MMC was found to be lower than that of AA2219. The smaller and finer grain size, improved hardness, reduction in the porosity level and uniform distribution of Si<sub>3</sub>N<sub>4</sub> particles are the various reasons for this. When the wt%

**Table 2** The corrosion behaviour of materials has been studied using Electrochemical workstation

Sample	Corrosion rate (mil/year)	Inhibition efficiency (%)
0 %	455.70	12.2
3 %	346.20	24.03
6 %	367.00	19.46
9 %	170.60	62.56

of Si<sub>3</sub>N<sub>4</sub> content increase the wear rate is found to be decreased with an increase in sliding velocity [26].

- The worn area shows a rough wear process, which is mainly the product of hard particulate exposure. In the case of AA2219/ Si<sub>3</sub>N<sub>4</sub> Composites, the particulate inhibits delamination progression, while the wear resistance is supplemental.
- The corrosion resistance of the matrix alloy was improved when Si<sub>3</sub>N<sub>4</sub> particles were added in a quantity of up to 9% by weight. The AA2219- Si<sub>3</sub>N<sub>4</sub> alloy matrix composite showed high corrosion resistance with corrosion rates of 367.00 mil/year for 6 wt% Si<sub>3</sub>N<sub>4</sub> and 170.60 mil/year 9 wt% Si<sub>3</sub>N<sub>4</sub>. Heat treatment of the composites and matrix alloy improved corrosion and wear resistance.

**Acknowledgements** Yes.

**Author Contributions** Equal contribution.

**Data Availability** I Can provide as per the request.

## Declarations

**Conflict of Interest** No Conflict of interest.

**Consent to Participate** Yes.

**Consent for Publication** Yes.

## References

1. Siddeshkumar NG, Shiva Shankar GS, Basavarajappa S (2015) Comparative study on dry sliding wear behaviour of metal matrix hybrid composites at room and high temperature conditions. *Int J Eng Res Adv Technol* 1:16–24
2. Dileep T, Srinivas PNS (2016) Enhancement of mechanical, microscopic and tribological properties of hybrid metal matrix composite reinforced with alumina, graphite and silicon carbide. *Int J Latest Eng Res Appl* 1:41–49
3. Jayasheel I, Hartil BR, Sridhar HR, Vitala, Jadhav PR (2015) Wear behavior of Al2219-TiC particulate metal matrix composites. *Am J Mater Sci* 5:34–37
4. Siddesh kumar NG, Ravindranath VM, Shiva Shankar GS (2014) Mechanical and wear behavior of aluminium metal matrix hybrid composites. *Procedia Mater Sci* 5:908–917
5. Rao VR, Ramanaiah N, Sarcar M, Moulana M (2016) Mechanical and tribological properties of AA7075–TiC metal matrix composites under heat treated (T6) and cast conditions. *JMRTEC* 5:1–7
6. Agnihotri R, Dagar S (2017) Mechanical properties of Al-SiC metal matrix composites fabricated by stir casting route. *Res Med Eng Sci* 2:1–6
7. Prince Jeya Lal L, Manigantan R, Suryanarayan CP (2016) Experimental study of wear rate coefficient of aluminium hybrid composites manufactured by stir casting technique 3:17–20
8. Suresh S, Shenbaga Vinayaga Moorthi N, Selvakumar N, Vettivel SC (2014) Tribological tensile and hardness behavior of TiB<sub>2</sub>



- reinforced aluminium metal matrix composite. *J Balk Tribol Assoc* 20:380–394
9. Manjunatha CJ, Narayana BVenkata (2019) Experimental analysis of mechanical properties of Aluminium Alloy 2219 reinforced with  $\text{Si}_3\text{N}_4$ . *Int J Innov Technol Explor Eng* 9:504–508
  10. Baradeswaran A, Elayaperumal A, Paulo Davim J (2013) Effect of B4c on mechanical properties and tribological behaviour of Al6061–B4c composites. *J Balk Tribol Assoc* 19
  11. Yusuf Kayali Y (2013) Wear and corrosion behaviour of borided and nitrided M2 high speed steel. *J Balk Tribol Assoc* 19:340–353
  12. Sulima I, Jaworska L, Wyzga P, Perek-Nowak M (2010) The influence of reinforcing particles on mechanical and tribological properties and microstructure of the steel–Tib2 composites. *J Achiev Mater Manuf Eng* 48:52–57
  13. Li P, Li Y, Wu Y, Ma G, Liu X (2012) Distribution of Tib2 particles and its effect on the mechanical properties of A390 alloy. *Mater Sci Eng A* 546:146–152
  14. Sreenivasan A, Paul Vizhian S, Shivakumar ND, Muniraju M, Raguraman M (2011) A study of micro structure and wear behavior of Tib2/Al metal matrix composites. *Solids Struct* 8:1–8
  15. Gunes I, Dalar A (2013) Effect of sliding speed on friction and wear behaviour of borided gear steels. *J Balk Tribol Assoc* 19:325–339
  16. Amit Sharma RM, Belokar SK (2018) *J Braz Soc Mech Sci Eng* 40: 294
  17. Suresha S, Sridhara BK (2010) *Compos Sci Technol* 70:1652
  18. Włodarczyk-Fligier A, Dobrzanski LA, Adamiak M (2007) Influence of heat treatment on corrosion resistance of PM composite materials. *J Achiev Mater Manuf Eng* 24:127
  19. Uvaraja VC, Natarajan N (2012) *J Miner Mater Charact Eng* 11:757
  20. Suresh S, Shenbaga Vinayaga Moorthi N, Vettivel SC, Selvakumar N, Jinu GR (2014) *Mater Sci Eng A* 612:15
  21. Veysel Erturun, sezer cetin, O Sahin (2020) Investigation of micro-structure of aluminium based composite material obtained by mechanical alloying. *Metals Mater Int* 1:9
  22. Sahin O, Erturun V (2018) The effect of magnesium additives on aluminum-based composites structure. *Powder Metall Met Ceram* 57:384
  23. Sreedev EP, Govind HK, Raj A, Adithyan PS, Narayan HA, Shankar KV, Balachandran M (2020) *Tribol Ind* 42:299
  24. Priyanka Muddamsetty LV, Radhika N (2016) *Tribol Ind* 38:108
  25. Reddy PV, Kumar GS, Krishnudu DM, Rao HR (2020) *J Bio-Tribo-Corros* 6:1–16
  26. Nunes PCR, Ramanathan LV (1995) Corrosion behavior of alumina-aluminum and silicon carbide-aluminum metal matrix composites. *Corrosion* 51:610
  27. Toptan F, Alves AC, Kerti I, Ariza E, Rocha LA (2013) Corrosion and tribocorrosion behavior of Al–Si–Cu–Mg alloy and its composites reinforced with B4C particles in 0.05 M NaCl solution. *Wear* 306:27
  28. Kolman DG, Butt DP (1997) Corrosion behavior of a novel SiC/Al<sub>2</sub>O<sub>3</sub>/Al composite exposed to chloride environments. *J Electrochem Soc* 144:3785
  29. Sun HH, Chen D, Li XF, Ma NH, Wang HW (2009) Electrochemical corrosion behavior of Al–Si alloy composites reinforced with in situ Tib2 particulate. *Mater Corros* 60:419
  30. Veysel Erturun M, Karamiş B (2016) Effects of reciprocating extrusion process on mechanical properties of AA 6061/SiC composites. *Trans Nonferrous Metals Soc China* 26:328

**Publisher's Note** Springer Nature remains neutral with regard to jurisdictional claims in published maps and institutional affiliations.